
sEMG Gesture Recognition with a Simple Model of Attention

David Josephs
 Southern Methodist University
 Dallas, TX 75205
 josephsd@smu.edu

Carson Drake
 Southern Methodist University
 Dallas, TX 75205
 drakec@smu.edu

Andy Heroy
 Southern Methodist University
 Dallas, TX 75205
 aheroy@smu.edu

John Santerre
 Southern Methodist University
 Dallas, TX 75205
 jsanterre@smu.edu

Abstract

Myoelectric control is one of the leading brain-machine-interfaces in the field of robotic prosthetics. We present our research in real-time surface electromyography (sEMG) signal classification, where our simple and novel attention-based approach now leads the industry, universally beating more complex, state-of-the-art models. Our model achieved an accuracy of 87% (class-balanced accuracy: 69%) using sEMG data and 91% (balanced accuracy: 74%) using both sEMG and accelerometer (IMU) data on NinaPro DB5, as well as 73% overall on NinaPro DB4, an improvement on both highly sophisticated deep learning and signal processing approaches. Notably, the representation of the data learned by the attention mechanism alone is powerful enough to yield an accuracy of 79% on DB5. NinaPro DB5 is a standard benchmark for sEMG gesture recognition and consists of 53 unique gestures, including finger gestures, wrist gestures, and functional grasping gestures. Our proposed methodology's model simplicity represents a compelling alternative to the convolutional neural network (CNN) approaches utilized in recent research.

1 Introduction

Electrophysiological studies of the nervous system are a core area of research in clinical neurophysiology, where scientists attempt to link electrical signals from the body to their physical manifestations. These studies include measuring brain waves (electroencephalography), comparison of sensory stimuli to electrical signals in the central nervous system (evoked potential), and the measure of electrical signals in skeletal muscles (electromyography) which is the focus of this paper.

When the nervous system uses electrical signals to communicate with a skeletal muscle, the myocytes (muscle cells) contract, causing physical motion. By measuring these electrical signals before they reach the myocytes we correlate signals to intended action. Such an approach allows for opportunities ranging from quantifying physical veracity to diagnosing neurodegenerative diseases. An example of the latter can be found in Akhmadeev et al. [2018], where electromyographic (EMG) signals were used to classify Multiple Sclerosis patients from healthy control subjects with 82% accuracy.

Current state-of-the-art myoelectric prosthetic limbs are capable of detecting and performing between 7 and 18 gestures [Geethanjali, 2016]. While there is great utility in such analysis, there remains considerable room for improvement. Our focus is on classifying signals used to dictate the motion of the hand.

Our key contribution is the utilization of an attention mechanism to transform the data for consumption by a relatively shallow neural network. Our work indicates that the key barrier holding back sEMG analysis is not limitations of interaction between the channels of signal (which might require more complicated network structure) but rather the process by which we work with the time aspect of the classification problem. Additionally, we extend this simple model to show that attention coupled with a simple neural network can produce research-leading results against standard benchmarks, both NinaPro DB4 and DB5. To our knowledge, models based purely on attention have never been shown to be effective tools for sEMG analysis. That, coupled with our adaptations (Mish activation, focal loss, and Ranger optimization), represent a new direction forward.

Specifically, we propose a feed-forward attention-based architecture for sEMG recognition and myoelectric control. Our simple attention mechanism, in conjunction with feed forward networks for time series classification data represents our main contribution. Using primarily the NinaPro DB5, as well as DB4, we demonstrate that a lightweight application of attention to sEMG data allows for benchmark leading results.

2 Background

2.1 Medical Background

Electromyography is the measure of electrical activity generated from skeletal muscles. We are particularly interested in brain mediated activity, where an electrical potential can be measured along the pathway of a signal originating in the central nervous system and transmitted to the muscular system. The motor control process can be modeled as an axon, which delivers signal to myocytes (muscle cells). The electrical signal causes the internal fibers of the muscle to contract to generate movement. The signals generated by these contractions, EMG signals, are measured in units of *Motor Unit Action Potential* (MUAP), which quantifies the difference in electrical potential between the inner and outer membranes of a myocyte. This is measured either through internal electrodes or electrodes on the surface of the skin (sEMG). We are particularly interested in sEMG, as although it is not as powerful as EMG, it is more practical and scalable (ready to be mass distributed) and less disruptive. These signals provide a measurement signals from several individual motor units. Though the sEMG signal has increased noise compared to intramuscular EMG, it presents a unobtrusive and easily configurable means of measuring the strength and volition of connection between brain and muscle, as well as intent [Ding et al., 2016]. This is of vital importance, as it allows an amputee whose limb does not biologically exist to still be able to make use of these signals.

2.2 Deep Learning for sEMG Classification

Much of the previous successful work in sEMG classification utilizes convolutional and recurrent neural networks to learn time, frequency, and time-frequency domain features. Shen et al. [2019] utilize all three of these domain features in conjunction with CNNs to classify the full NinaPro DB5 data set with 75% accuracy. Côté-Allard et al. [2019] builds off the work of Atzori et al. [2016], using wavelet transforms (a time-frequency domain transformation) and periodograms (a frequency domain transformation) in conjunction with transfer learning and convolutional networks to obtain an accuracy of 69% over the wrist gesture subset of NinaPro DB5. Wei et al. [2019] use multi-view CNNs on a set of classical time and frequency domain features and IMU data to score 91% on the wrist and functional gestures of NinaPro DB5. Hu et al. [2018] looked to build a more robust representation of the time features of this data set using several CNN-RNN combinations, combined using attention mechanisms. Rahimian et al. [2020] takes a novel approach to solve the time domain information problem, using a new separable depth wise convolutional architecture. Parallel to this, Wei et al. [2019], Ketykó et al. [2019], and Du et al. [2017] utilize domain adaptation techniques to help sEMG classifiers generalize not only across time, but across people, while Côté-Allard et al. [2019], Zhai et al. [2017], and Zia ur Rehman et al. [2018] also examine day-to-day calibration techniques, for practical use in amputees.

One of the large problems in this space is determining how to represent the data in a manner in which neural networks can learn both spatial and temporal features. The literature indicates that there is a trade off between the complexity of the network and the complexity of preprocessing and feature extraction mechanisms [Hu et al., 2018, Rahimian et al., 2020]. We aim to show that with a

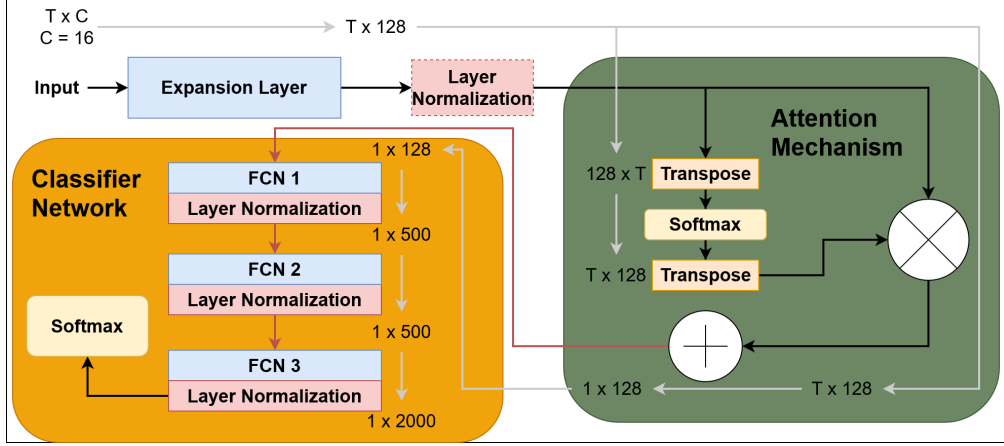


Figure 1: A diagram of our simple attention-based model. Note that red connections indicate dropout, and layer normalization is indicated as it contributed to our best results. The dimensions of a single window of input before and after each layer are shown, connected by gray arrows. FCN stands for “fully connected network”.

simple architecture, minimal preprocessing, and no feature extraction, we can accurately capture the relationship between sEMG and motion.

Accordingly, we explore adapting the language modeling notion of attention for sEMG analysis. We show that a feed-forward simplification of attention is capable of learning a time domain representation of multichannel sEMG data. This approach manages to avoid not only the training and gradient issues of RNNs, but also the difficulty of data representation met by CNNs, performing well on near raw sEMG signal. The simplified attention mechanism discussed in Raffel and Ellis [2015] is expanded upon, for use with purely feed-forward networks. Raffel and Ellis [2015] propose two approximations of a simple attention function, a simple sum across time as well as:

$$\alpha_t = \text{softmax}(\tanh(W_{hc}h_t + b_t)). \quad (1)$$

Where α_t is the attention score at timestep t , h_t is the output of the previous layer of the network, and W_{hc} and b_t are learned weights and biases. Raffel and Ellis [2015] demonstrate that on toy problems, feed forward networks can use this mechanism to model sequences in which order is not important.

3 Modeling

Our attention-based model architecture, shown in Figure 1, consists of two parts: the expansion and attention mechanism, and a classifier network. The data is fed into an expansion layer, which learns to expand the input data from a window of C channels and T timesteps to a matrix of T timesteps and 128 channels. As seen in Table 3, the nature of this layer, fully connected or convolutional, is not important. This matrix is then processed by the feed-forward attention mechanism seen in Figure 1, resulting in a feature vector of 128 values. These are fed into the classification network, which consists of a set of standard, fully connected network (FCN) layers. The classifier is made up of two 500 node fully connected layers, one 2000 node fully connected layer, and a softmax layer, as shown in Figure 1. All parts of the classifier are separated by dropout connections.

Initially, we followed a CNN based approach in conjunction with attention. This had little effect on accuracy relative to a simple fully connected layer with attention. We include the specifications of the CNN here for clarity to further reinforce the value of the attention layer alone. We used a single, 1-dimensional convolutional layer with a kernel size of 3 and same padding at the bottom of the network in conjunction with layer normalization between each layer.

3.1 Attention Mechanism

The attention mechanism works as follows: First time series data processed by the previous layer, $h \in \mathbb{R}^{T \times C}$, where T represents timesteps and C represents features or channels, is inputted. h is

transposed into an $C \times T$ matrix. In h^T an observation at a single row represents all timesteps of that feature or channel. For example, row h_i^T represents the time series produced by the channel $C = i$. This matrix is then fed in row by row to a standard, fully connected layer using the softmax activation function, resulting in a $C \times T$ matrix, α . This can be expressed as:

$$\alpha = \text{softmax}(W_{hc}h^T + b_{tc}). \quad (2)$$

Where $\alpha \in \mathbb{R}^{C \times T}$ is an attention matrix and $W_{hc} \in \mathbb{R}^{T \times C}$, $b \in \mathbb{R}$ are learned weights and biases across time. For clarity, the entry α_{ij} is the attention score for timestep j at channel i . Thus, α^T represents a matrix containing a learned temporal mask for each channel. By taking the Hadamard product of α^T and h , and summing across time, we calculate a vector $c \in \mathbb{R}^{1 \times C}$, analogous to a context vector.

$$g = \alpha^T \circ h, g \in \mathbb{R}^{T \times C} \quad (3)$$

$$c = \sum_{t=1}^T g, c \in \mathbb{R}^{1 \times C} \quad (4)$$

This naive attention mechanism proves surprisingly capable of learning expressive representations of multi-channel signal. More complicated approaches should lead to greater gains, but the baseline attention model proves more than sufficient for demonstration purposes.

3.2 Training and Implementation Details

Each model was trained for 55 epochs with a batch size of 128, and a learning rate annealed from $1 * 10^{-3}$ to $1 * 10^{-5}$. We chose 55 epochs because after 45-55 epochs, the model did not improve any further.

Rather than using the Rectified Linear Unit (ReLU) activation function, all layers use the “Mish” activation function, proposed by Misra [2019], with the idea of reaching a good optima in fewer iterations. Instead of optimizing the network with Adam or SGD, the model was optimized using the Ranger optimizer. The Ranger optimizer consists of two components: Rectified Adam (RAdam) and Lookahead. The RAdam algorithm represents an improvement over the Adam optimizer in that it does not require a “warm up period”. This allows the model to be trained to an optima much faster [Liu et al., 2019]. The Lookahead algorithm works in conjunction with a primary optimizer. The primary optimizer calculates weights as it normally does, and then the Lookahead optimizer explores the loss landscape near the calculated weights. This allows for even faster convergence to an optima [Zhang et al., 2019]. The combination of Lookahead and RAdam is the Ranger optimizer used in this paper [Tong et al., 2019]. The learning rate follows a delayed cosine annealing schedule. For the first 5 epochs, the model trains at a high learning rate, and is subsequently annealed over the course of 50 epochs to a low learning rate. This training process takes between 3 and 4 hours, or about half the time to train a similarly complex convolutional or recurrent network. For regularization, dropout with a rate of 0.36 is applied to all layers in the classification network.

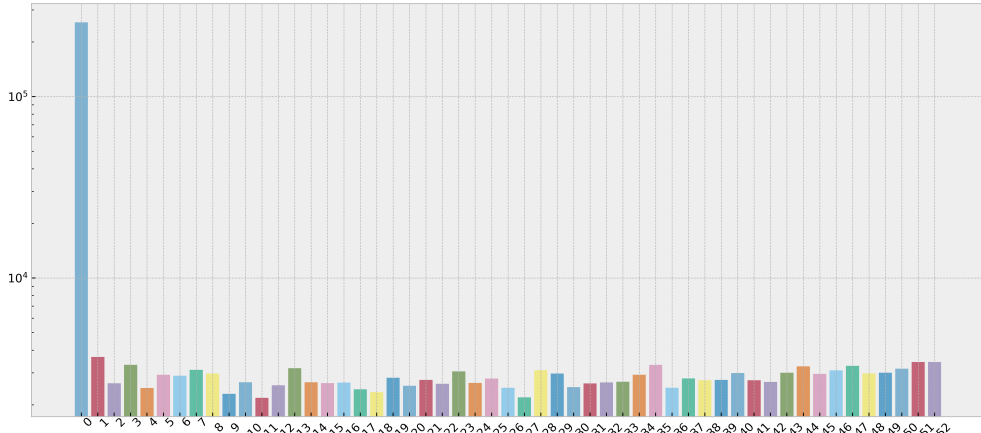


Figure 2: Counts of gestures in DB5, on a log scale.

A significant issue with laboratory-collected sEMG data is the large class imbalance present, as seen in Figure 2. Most of the time, the hand is at rest, as each repetition of each exercise is followed by 3 seconds of rest. This is analogous to the real world, as we do not constantly move our hands; however, this complicates the classification task. In NinaPro DB5, there is over 30 times as much rest as any of the other 52 gestures. Several measures were taken to combat this. First, instead of training with standard cross-entropy, all models were trained using the focal loss function from computer vision, which weights easy to classify examples (rest) less than difficult examples when calculating the gradients. Secondarily, a novel data augmentation scheme was implemented, adding noise with a spectrum of Signal-To-Noise Ratios. For each window passed in, a random SNR between 1 and 30 (with 30 being more likely than 1) is selected, and SNR-preserving noise is calculated and added to the window. Due to the strong imbalance in the data, rest is not augmented. This is analogous to oversampling the minority class with synthetic data [Johnson and Khoshgoftaar, 2019]. After between 30 and 40 epochs, the model will have seen an the same amount of unique samples of each class as it will have seen rest.

4 Data

The MYO arm band [Visconti et al., 2018] is a low-cost, \$200, low-frequency sEMG device. While other research grade devices achieve higher sampling frequencies, they are also very dependent on placement configuration and operator calibration. A critical requirement for a consumer grade sensor setup is ease of configuration, this is one advantage of consumer grade hardware, because exact positioning of the electrodes cannot be assured, the algorithmic approach taken must be more robust. Thus choosing lower grade hardware puts greater emphasis on the necessity of algorithmic analysis and prepossessing data which is easily scale-able rather then expensive hardware and technical experience.

The NinaPro [Atzori and Müller, 2015] project represents the largest data collection effort in the sEMG space, consisting of 10 large databases collected from both amputees and intact subjects using various sensors. The main benchmark used in this paper is the NinaPro DB5, or the “Double MYO” dataset. The NinaPro DB5 uses two MYO armbands, offset in both position and angle, collecting 16 channels of sEMG data, as well as triaxial accelerometer (Inertial Measurement Unit or IMU) data, at 200 Hz. Information on the test subjects such as arm circumference, gender, and age can be found in Pizzolato et al. [2017]. Additionally, some ana was done with NinaPro DB4 data set which utilized the same experimental design but collected using 12 sensors at 2 kHz [Pizzolato et al., 2017].

For both DB5 and DB4, there are 53 unique gestures measured, collected over 10 subjects. The subjects perform six repetitions of each exercise, buffering each exercise repetition with three seconds of rest. The databases contain 12 fine finger gestures, 17 fine wrist gestures, 23 functional (grasping) gestures, and rest. This data looks like a 16 channel time series with approximately 600000 rows per subject. Each of the 10 individuals performed 318 gestures. In DB5, the signal is collected at 200 Hz, the sampling frequency of the MYO armband. DB4 collects 12 channels of sEMG at 2 kHz using Cometa differential electrodes on the same experimental design, providing a good high frequency comparison to DB5.

The data was processed as follows. First, following the precedent set by Côté-Allard et al. [2019], the raw data stream is broken into 260 millisecond windows, with 235 milliseconds of overlap. This window size was chosen in part due to the work of Smith et al. [2011] and Hudgins et al. [1993], who determined that the absolute largest window size for use in a prosthetic limb lies somewhere between 250 and 300 milliseconds. Windows which contain multiple gestures (generally rest and another gesture) are labeled using the first gesture, meaning a window which is mostly rest at the beginning and then a grabbing gesture will be classified as rest, and a window which is mostly a grabbing gesture followed by a rest is classified as a grabbing gesture. Windows containing multiple repetitions were discarded. Next, the data is rectified, which exposes more information on the firing rate of the motor units [Myers et al., 2003], and artifacts are removed with a 20 Hz high-pass Butterworth filter. The order of these two steps is important, as the rectification alters the power spectrum of the signal, and thus alters the results of filter. Finally, we smooth the data with a moving average filter. This brings T , the number of timesteps in a window, down from 52 to 38 and 520 to 381 in DB5 and DB4 respectively. For all trials, the third repetition was used to tune parameters and the fifth as an unseen holdout set. The fifth repetition is commonly used in testing [Atzori et al., 2016, Wei et al., 2019, Pizzolato et al., 2017].

5 Results



Figure 3: Accuracy calculated using inter-session cross validation, using 5 repetitions to train and one to test, for each repetition. We see fairly consistent results across time.

Using an NVIDIA Tesla V100 on CentOS Linux, provided by the SMU Center for Scientific Computing, an accuracy of 87% (balanced accuracy 69%) was achieved on NinaPro DB5, across all 53 classes. By including the recorded IMU(accelerometer) data, the accuracy increased to 91%, and balanced accuracy to 74%. This can be seen in Figure 3, as well as a strong 73% accuracy on NinaPro DB4, a good high frequency reference. All models are implemented in Tensorflow and are available at <https://github.com/josephsdavid/attentionsemg>.

Table 1: Comparison to the current state-of-the-art. Items in **bold** mark benchmark-leading results. An asterisk(*) denotes our contribution. Each model was trained and evaluated 30 times on the same holdout set with different seeds, with consistent results (95% confidence interval: ± 0.0004).

(a) DB5, all gestures	(b) DB5, wrist and functional gestures
Model	Accuracy
Attention model with IMU*	91%
Attention model*	87%
Shen et al. [2019]	75%
<hr/>	
(c) DB5, just wrist gestures, no IMU	(d) DB4, all gestures
Model	Accuracy
Attention model*	89%
Côté-Allard et al. [2019]	69%
Chen et al. [2020]	67%
Wu et al. [2018]	62%
<hr/>	
<hr/>	
Model	Accuracy
Attention model*	73%
Pizzolato et al. [2017]	69%
Wei et al. [2019]	60%

In Table 1, we see how our simple attention-based model compares with the state-of-the-art in sEMG classification. Although our model is relatively naive and straightforward our results are benchmark leading. As we have noted elsewhere, we see that even a simple attention based model can encode temporal and spatial features into a compressed representation connected to softmax layer was able to perform surprisingly well (79%, as seen in Table 5). This alone represents a strong result. We were able to increase accuracy gains with a distinct uptick of 8% by training a fully connected classifier network. This indicates that while the representation of data learned in attention is useful there is still value and potential in using neural networks trained to work in this newly encoded space.

6 Discussion

In order to better understand and clarify the source of our results, we performed an exhaustive layer by layer analysis of the proposed model. We used three metrics to assess these experiments: accuracy, class-balanced accuracy, and Matthews Correlation Coefficient (MCC) [Baldi et al., 2000, Chicco and Jurman, 2020]. The MCC, formerly known as Pearson’s Phi, represents the correlation coefficient between true and predicted labels, using a confusion matrix. In the case of imbalanced data, it has the useful property of going to zero when a class is completely missed. Given the imbalances typically present in laboratory-collected sEMG data (see Figure 2), we believe the MCC is a more appropriate metric for this data.

Table 2: Reference values for metrics. The weighted random and unweighted random values are an average of 1000 trials.

	Weighted Random	Unweighted Random	All Zeros	All Ones
Accuracy	0.406176	0.018954	0.635	0.009
Balanced Accuracy	0.018953	0.018876	0.019	0.019
MCC	0.000028	-0.000006	0.000	0.000

In Table 2 we have provided four naive baseline models to provide more context to our results. These consist of two random models, one with equally weighted class distribution and one with class distribution reflected in NinaPro DB5, and two homogeneous models. For the homogeneous models we chose zero and one to demonstrate what expected results would be if all inputs were classified as the most common class, rest, and contrast those results with a model that classified all with one of the other non rest classes.

Table 3: Experiments on the expansion layer of the network.

Model	No. Parameters	Accuracy	Balanced Accuracy	MCC
Fully connected	$1.44 * 10^6$	87.17%	69.83%	0.78
Conv1D	$1.44 * 10^6$	87.15%	69.70%	0.78
Frozen fully connected layer	$1.43 * 10^6$	84.18%	62.90%	0.73
No expansion	$1.37 * 10^6$	77.80%	41.79%	0.59

We first try to understand the role of the expansion layer. In Table 3, we conduct four experiments: first, a fully connected layer is used for the expansion layer; second, 1 dimensional convolutions with kernel size 3; third, a fully connected but frozen layer; and fourth, the raw data is fed directly into the attention layer. We find that there is no significant difference between the convolutional and fully connected expansion layers, but the presence of the expansion layer does have an effect. This suggests that the allocation of space is important, and allows the network to learn a more efficient representation. We also believe this suggests that the temporal properties of the data are more important than the spacial properties, as the fully connected layer assumes independence across time while the attention layer assumes independence across channels.

Table 4: Experiments on the attention mechanism.

Model	No. Parameters	Accuracy	Balanced Accuracy	MCC
Final fully connected model	$1.44 * 10^6$	87.17%	69.83%	0.78
Raffel attention	$1.44 * 10^6$	86.82%	69.29%	0.77
Temporal sum	$1.44 * 10^6$	86.40%	67.82%	0.77

In Table 4, we see that a very slight decrease in accuracy occurs by replacing the attention mechanism with the two alternatives proposed in Raffel and Ellis [2015]; that mentioned in Equation 1, and a sum across time. Although the accuracies appear similar, the sum across time approximation of attention yielded a noticeably lower class-balanced accuracy.

Table 5: Experiments on the classifier network.

Model	No. Parameters	Accuracy	Balanced Accuracy	MCC
Final fully connected model	$1.44 * 10^6$	87.17%	69.83%	0.78
Small classifier net	$1.0 * 10^5$	79.79%	47.81%	0.65
No classifier net	$1.4 * 10^4$	79.71%	46.58%	0.64

In Table 5 we investigate the influence of the classifier network, with two more experiments. First, we completely remove the classifier network, feeding the output of attention into a single softmax layer. We then add a small classifier network, consisting of a single layer with 500 nodes. We see that without a classifier network, we still retain about 80% of our accuracy. Table 2 shows that this is not due to chance, but represents a powerful result. By adding a single 500 node classifier network we don’t see a increase in accuracy but even with a minimal increase in neural network depth to three layers we find that our accuracy increases. This suggests that we are learning to encode spatiotemporal features of the data into a low-dimensional representation with our attention mechanism, and the classifier network is disentangling that representation.

Table 6: Experiments on our minor adaptations.

Model	No. Parameters	Accuracy	Balanced Accuracy	MCC
Final fully connected model	$1.44 * 10^6$	87.17%	69.83%	0.78
No layer normalization	$1.43 * 10^6$	86.94%	69.38%	0.78
Relu instead of Mish	$1.44 * 10^6$	86.60%	64.08%	0.77

Finally, we examine the roles of layer normalization and the Mish activation function. We see in Table 6, that these did have a rather minor effect on overall accuracy but useful net positive effect on our balanced accuracy.

All models and experiments were trained using the exact same hyperparameters, mentioned in section 3, in order to avoid any confounding factors.

7 Conclusion

Our algorithm yields a benchmark leading result from a comparatively lightweight and easy to train neural network. Rather than starting with a strong set of priors about how the channels, time, and signal will interact, we demonstrate our results by providing sufficient space to expand the channels and then condense using an attention layer onto a lower dimensional representation. That this representation only requires a simple three layer feed-forward neural network, implies that the bulk of the computational heavy lifting was achieved in the attention layer. One implication is that the first complexity of sEMG analysis is learning a suitable representation space. An intuitive way of understanding this is that sEMG sensors are not surgically attached, and therefore sensors shift from individual to individual. Addressing this simplifies the computational needs of the final neural network. The implication is that the attention layer is finding an invariant representation with respect to the targeted 53 gestures, as evidenced by the performance of the classifier-free model. Our research points strongly toward the further exploration of attention-based models, a promising avenue for future research in not only the sEMG space, but also electrophysiological signals in general.

8 Broader Impact

Interaction devices that allow computers to capture the intention of humans include some of the earliest demonstrations of computer science. Active physical manipulations of objects (keyboards, mice, joysticks) dominate the space, while direct cognitive devices occupy the greatest hope for capturing human intent. We thus separate our discussion into three categories: direct implication, basic research, and core machine learning.

8.1 Direct Implication

The goal of sEMG analysis is to provide and utilize a direct measurement of intention [Ding et al., 2016], and associate it with its physical manifestation. The value of such an approach cannot be overstated. Potential applications of capturing intent and physical motion include therapeutic use cases where intentions are available but physical deficits (amputation, neuromuscular disease) prevents the final action from occurring. Additionally human augmentation such as robotic exoskeletons would benefit directly from such an approach as it would not require the mechanical movement of objects. Human Computer Interaction researchers are actively looking for opportunities to expand the expressiveness and responsiveness of interaction approaches. While keyboards, mice and most recently touch continue to be the most commonly utilized frameworks for interaction researchers understand that we must continue to look for more opportunities.

8.2 Basic Research

From a basic research perspective the capturing of signals offers the potential of correlation of distal signals with signaling that occurs closer to the brain stem. Understanding the extent to which signal interpretation is feasible in particular clinical conditions can shed light on individual cases for diagnostic reasons. Additionally such analysis may provide useful insight into the origins of certain neuromuscular diseases. sEMG, due to its low cost of entry may provide analysis opportunities for otherwise marginalized communities who typically do not have access to more complicated diagnostic tools.

8.3 Core Machine Learning

The computational approach driven by our analysis implies that the most fundamental approach to understanding sEMG signals is only beginning to be understood. Consequently our contribution of bringing attention into this particular domain has implications on future work related to signal processing and machine learning in the human body. Our central thesis implies that the problem of disentangling sEMG signals isn't a question of the representation being problematic but rather simply identifying the right temporal scope to operate on.

We believe the impact of this vein of research has the potential to clinically impact 10's millions of individuals, while the commercial implications of a large scale adoption of sEMG interaction device would be likely to impact more than 100's of millions. Despite this optimism, there are hurdles. Our research is only one stepping stone, and accuracies are not yet sufficient for widespread commercial adoption. Despite the fact clinical settings have lower expectation and greater willingness to struggle with technology to achieve an end result. We recognize that our proposal is an academic advancement that will require extensive testing for deployment.

Despite these caveats, we are excited and enthused about the opportunities this research present and look forward to its continued exploration.

References

- K. Akhmadeev, A. Houssein, S. Moussaoui, E. A. Høgestøl, I. Tutturen, H. F. Harbo, S. D. Bø-Haugen, J. Graves, D.-A. Laplaud, and P.-A. Gourraud. Svm-based tool to detect patients with multiple sclerosis using a commercial emg sensor. *2018 IEEE 10th Sensor Array and Multichannel Signal Processing Workshop (SAM)*, pages 376–379, 2018.
- M. Atzori and H. Müller. The ninapro database: a resource for semg naturally controlled robotic hand prosthetics. In *2015 37th Annual International Conference of the IEEE Engineering in Medicine and Biology Society (EMBC)*, pages 7151–7154. IEEE, 2015.
- M. Atzori, M. Cognolato, and H. Müller. Deep learning with convolutional neural networks applied to electromyography data: A resource for the classification of movements for prosthetic hands. *Frontiers in Neurorobotics*, 10, Jul 2016. doi: 10.3389/fnbot.2016.00009.
- P. Baldi, S. Brunak, Y. Chauvin, C. A. F. Andersen, and H. Nielsen. Assessing the accuracy of prediction algorithms for classification: an overview . *Bioinformatics*, 16(5):412–424, 05 2000.

ISSN 1367-4803. doi: 10.1093/bioinformatics/16.5.412. URL <https://doi.org/10.1093/bioinformatics/16.5.412>.

L. Chen, J. Fu, Y. Wu, H. Li, and B. Zheng. Hand gesture recognition using compact cnn via surface electromyography signals. *Sensors*, 20(3):672, 2020.

D. Chicco and G. Jurman. The advantages of the matthews correlation coefficient (mcc) over f1 score and accuracy in binary classification evaluation. *BMC Genomics*, 21(1), Feb 2020. doi: 10.1186/s12864-019-6413-7.

U. Côté-Allard, C. L. Fall, A. Drouin, A. Campeau-Lecours, C. Gosselin, K. Glette, F. Laviolette, and B. Gosselin. Deep learning for electromyographic hand gesture signal classification using transfer learning. *IEEE Transactions on Neural Systems and Rehabilitation Engineering*, 27(4): 760–771, April 2019. ISSN 1558-0210. doi: 10.1109/TNSRE.2019.2896269.

Q. Ding, A. Xiong, X. Zhao, and J. Han. A review on researches and applications of semg-based motion intent recognition methods. *Acta Automatica Sinica*, 42(1):13–25, 2016.

Y. Du, W. Jin, W. Wei, Y. Hu, and W. Geng. Surface EMG-based inter-session gesture recognition enhanced by deep domain adaptation. *Sensors*, 17(3):458, 2017.

P. Geethanjali. Myoelectric control of prosthetic hands: state-of-the-art review. *Medical Devices: Evidence and Research*, Volume 9:247–255, 2016. doi: 10.2147/mder.s91102.

Y. Hu, Y. Wong, W. Wei, Y. Du, M. Kankanhalli, and W. Geng. A novel attention-based hybrid cnn-rnn architecture for semg-based gesture recognition. *PloS one*, 13(10), 2018.

B. Hudgins, P. Parker, and R. N. Scott. A new strategy for multifunction myoelectric control. *IEEE Transactions on Biomedical Engineering*, 40(1):82–94, Jan 1993. ISSN 1558-2531. doi: 10.1109/10.204774.

J. M. Johnson and T. M. Khoshgoftaar. Survey on deep learning with class imbalance. *Journal of Big Data*, 6(1):27, 2019.

I. Ketykó, F. Kovács, and K. Z. Varga. Domain adaptation for semg-based gesture recognition with recurrent neural networks. In *2019 International Joint Conference on Neural Networks (IJCNN)*, pages 1–7. IEEE, 2019.

L. Liu, H. Jiang, P. He, W. Chen, X. Liu, J. Gao, and J. Han. On the variance of the adaptive learning rate and beyond. *arXiv preprint arXiv:1908.03265*, 2019.

D. Misra. Mish: A self regularized non-monotonic neural activation function. *arXiv preprint arXiv:1908.08681*, 2019.

L. Myers, M. Lowery, M. Omalley, C. Vaughan, C. Heneghan, A. S. C. Gibson, Y. Harley, and R. Sreenivasan. Rectification and non-linear pre-processing of emg signals for cortico-muscular analysis. *Journal of Neuroscience Methods*, 124(2):157–165, 2003. doi: 10.1016/s0165-0270(03)00004-9.

S. Pizzolato, L. Tagliapietra, M. Cognolato, M. Reggiani, H. Müller, and M. Atzori. Comparison of six electromyography acquisition setups on hand movement classification tasks. *PLOS ONE*, 12: e0186132, 10 2017. doi: 10.1371/journal.pone.0186132.

C. Raffel and D. P. Ellis. Feed-forward networks with attention can solve some long-term memory problems. *arXiv preprint arXiv:1512.08756*, 2015.

E. Rahimian, S. Zabihi, S. F. Atashzar, A. Asif, and A. Mohammadi. Xceptiontime: Independent time-window xceptiontime architecture for hand gesture classification. In *ICASSP 2020-2020 IEEE International Conference on Acoustics, Speech and Signal Processing (ICASSP)*, pages 1304–1308. IEEE, 2020.

S. Shen, K. Gu, X. Chen, M. Yang, and R. Wang. Movements classification of multi-channel semg based on cnn and stacking ensemble learning. *IEEE Access*, 7:137489–137500, 2019.

L. H. Smith, L. J. Hargrove, B. A. Lock, and T. A. Kuiken. Determining the optimal window length for pattern recognition-based myoelectric control: Balancing the competing effects of classification error and controller delay. *IEEE Transactions on Neural Systems and Rehabilitation Engineering*, 19(2):186–192, Apr 2011. doi: 10.1109/tnsre.2010.2100828. URL <http://dx.doi.org/10.1109/TNSRE.2010.2100828>.

Q. Tong, G. Liang, and J. Bi. Calibrating the adaptive learning rate to improve convergence of adam. *arXiv preprint arXiv:1908.00700*, 2019.

P. Visconti, F. Gaetani, G. Zappatore, and P. Primiceri. Technical features and functionalities of myo armband: An overview on related literature and advanced applications of myoelectric armbands mainly focused on arm prostheses. *International Journal on Smart Sensing and Intelligent Systems*, 11:1–25, 06 2018. doi: 10.21307/ijssis-2018-005.

W. Wei, Q. Dai, Y. Wong, Y. Hu, M. Kankanhalli, and W. Geng. Surface-electromyography-based gesture recognition by multi-view deep learning. *IEEE Transactions on Biomedical Engineering*, 66(10):2964–2973, 2019.

Y. Wu, B. Zheng, and Y. Zhao. Dynamic gesture recognition based on lstm-cnn. In *2018 Chinese Automation Congress (CAC)*, pages 2446–2450, 2018.

X. Zhai, B. Jelfs, R. H. Chan, and C. Tin. Self-recalibrating surface emg pattern recognition for neuroprosthesis control based on convolutional neural network. *Frontiers in neuroscience*, 11:379, 2017.

M. Zhang, J. Lucas, J. Ba, and G. E. Hinton. Lookahead optimizer: k steps forward, 1 step back. In *Advances in Neural Information Processing Systems*, pages 9593–9604, 2019.

M. Zia ur Rehman, A. Waris, S. O. Gilani, M. Jochumsen, I. K. Niazi, M. Jamil, D. Farina, and E. N. Kamavuako. Multiday emg-based classification of hand motions with deep learning techniques. *Sensors*, 18(8):2497, 2018.